

CCIN: Compositional Conflict Identification and Neutralization for Composed Image Retrieval

Supplementary Material

1. More Experimental Details

In this section, we provide further details of the proposed CCIN in several aspects.

Network Architecture. The Adaptive Fusion Module is specifically designed to enable efficient multi-modal integration, which incorporates a Multi-Layer Perceptron (MLP) and a Sigmoid activation function to dynamically fuse diverse inputs. The detailed design of this module is presented in the left panel of Figure 8. In parallel, the Instruction-aware Q-Former extends the conventional Q-Former architecture by incorporating textual instructions as an additional input. This extension enables the module to focus on extracting task-specific features from images, which align with the semantic context provided by the instructions. The detailed architecture of this module is shown in the right panel of Figure 8.

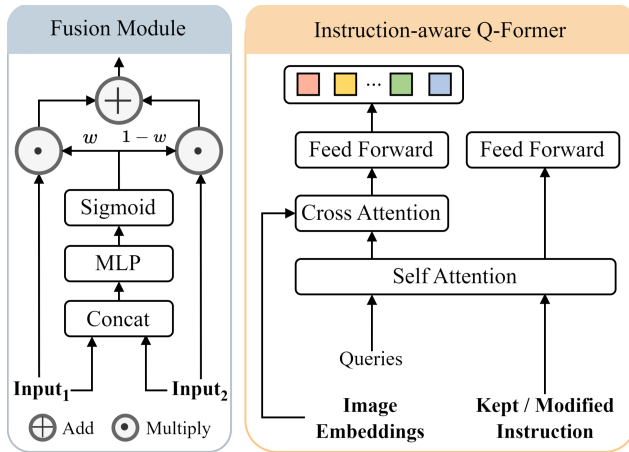


Figure 8. The architectural details of the Adaptive Fusion Module and the Instruction-aware Q-Former.

Loss Function Details. During training, we employ three distinct loss functions (\mathcal{L}_{ITC} , \mathcal{L}_{WRT} , and \mathcal{L}_{OPR}) to optimize the model and improve CIR performance.

Contrastive Learning Loss \mathcal{L}_{ITC} :

$$\mathcal{L}_{\text{ITC}} = -\frac{1}{B} \sum_i \log \frac{\exp(\mathbf{f}_{\text{query}} \mathbf{f}_{\text{tar}}^T)}{\sum_{j \in \mathcal{B}} \exp(\mathbf{f}_{\text{query}} \mathbf{f}_{\text{tar}}^T)}, \quad (9)$$

where B denotes the batch size, while $\mathbf{f}_{\text{query}}$ and \mathbf{f}_{tar} represent the composed query representation and the target image representation, respectively.

Weighted Regularization Triplet Loss \mathcal{L}_{WRT} :

$$w_{ij}^p = \frac{\exp(d_{ij}^p)}{\sum_{d_{ij}^p \in \mathcal{P}_i} \exp(d_{ij}^p)}, w_{ik}^n = \frac{\exp(-d_{ik}^n)}{\sum_{d_{ik}^n \in \mathcal{N}_i} \exp(-d_{ik}^n)}, \quad (10)$$

$$\mathcal{L}_{\text{WRT}}(i) = \log(1 + \exp(\sum_j w_{ij}^p d_{ij}^p - \sum_k w_{ik}^n d_{ik}^n)), \quad (11)$$

where (i, j, k) represents a hard triplet within each training batch. p_i and n_i denotes the positive and negative set for anchor i , respectively. d_{ij}^p/d_{ik}^n denotes the distance between a positive/negative sample pair.

Orthogonal Projection Regularization Loss \mathcal{L}_{OPR} :

$$\tilde{\mathbf{f}}_{\text{con}} = W_1(\mathbf{f}_{\text{con}}), \tilde{\mathbf{f}}_{\text{tar}} = W_2(\mathbf{f}_{\text{tar}}), \quad (12)$$

$$\mathcal{L}_{\text{OPR}} = \alpha \cdot \frac{\|W_1 W_2^T\|_F}{\|W_1\|_F \cdot \|W_2\|_F} + \beta \cdot \frac{\|\tilde{\mathbf{f}}_{\text{con}} \tilde{\mathbf{f}}_{\text{tar}}^T\|_F}{\|\tilde{\mathbf{f}}_{\text{con}}\|_F \cdot \|\tilde{\mathbf{f}}_{\text{tar}}\|_F}, \quad (13)$$

where \mathbf{f}_{con} and \mathbf{f}_{tar} donate the conflicting attribute feature and the target image feature, while $\|\cdot\|_F$ represents the Frobenius norm, respectively. Regularizing the projection matrix rather than the original features helps preserve feature information and prevent overfitting.

Dataset Details. In the experimental setup, we utilize three benchmark datasets: FashionIQ [48], CIRR [27], and Shoes [16]. The statistics details of these datasets, including the number of triplets, images, and their respective domains, are summarized in Table 7.

Dataset	Triplets	Images	Domain
FashionIQ [48]	30,134	77,684	Fashion
CIRR [27]	36,554	21,552	Natural
Shoes [16]	10,751	14,764	Fashion

Table 7. Existing Composed Image Retrieval (CIR) datasets, FashionIQ [48], CIRR [27], and Shoes [16], respectively.

Training Details. Following [2], the input images are pre-processed to a fixed resolution of 224×224 . And the batch size is consistently set to 64 for experiments on FashionIQ [48], CIRR [27], and Shoes [16] datasets.

2. More Visualization Results

In this section, we provide more visualization results of the proposed CCIN in several aspects.

Retrieval Results. To further evaluate the efficacy of CCIN, we perform additional comparative experiments against SPRC [2], which lacks mechanisms for addressing

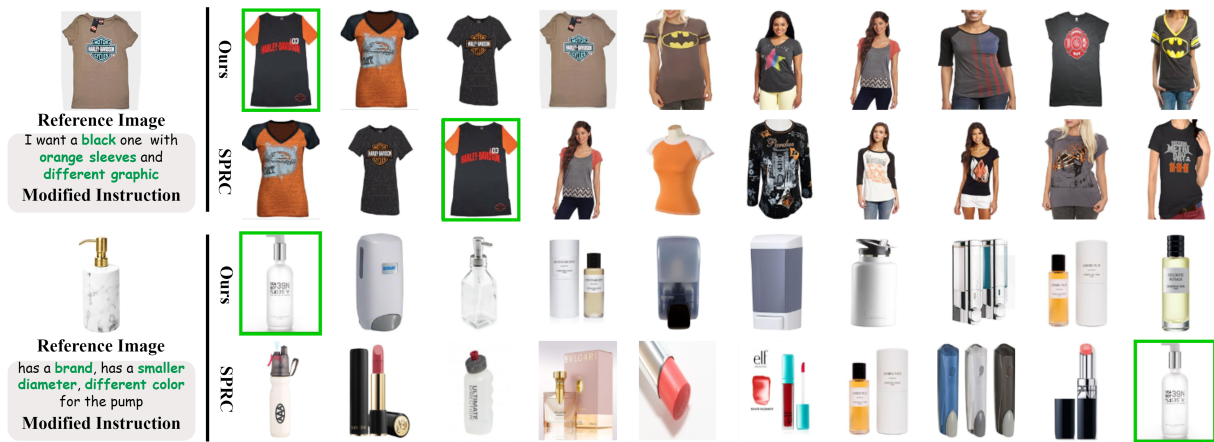


Figure 9. More qualitative results comparing SPRC [2] with the proposed method, with respect to Recall@1 metric on FashionIQ [48] and CIRR [27] datasets. The reference image and modified instruction are displayed on the left, while the retrieval rank is presented on the right. Correct matches are highlighted within green rectangles, respectively.

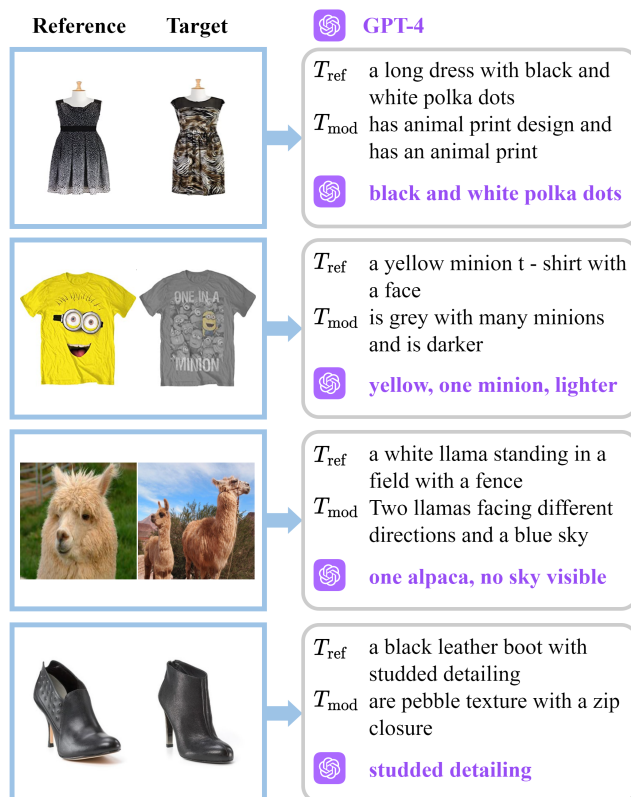


Figure 10. More qualitative results of CCI on three datasets [16, 27, 48]. Specifically, T_{ref} and T_{mod} denote the reference image caption and the modified instruction. The conflict identification results are highlighted in purple, respectively.

compositional conflicts. More visualization results on FashionIQ [48] and CIRR [27] are presented in Figure 9.

Conflict Identification Results. To demonstrate the effectiveness of CCI, we provide additional visualizations

Type	FashionIQ	CIRR	Shoes	Type	FashionIQ	CIRR	Shoes
	Mean	Mean	Mean		Mean	Mean	Mean
Cos	64.04	81.02	59.26	Direct	62.90	79.20	59.01
Ours	64.59	81.66	59.42	Ours	64.59	81.66	59.42

Table 8. Left: Comparison with using cosine similarity loss (Cos) to regularize original feature distances. Right: Comparison with directly (Direct) using LLMs to formulate target instruction (reference caption + modified instruction).

of conflict identification results from the FashionIQ [48], CIRR [27], and Shoes [16] datasets, as illustrated in Figure 10.